Supporting Information for

Identification of a Metastable Uranium Metal–Organic Framework Isomer Through Non-Equilibrium Synthesis

Sylvia L. Hanna[1], Tekalign T. Debela[3], Austin M. Mroz[3], Zoha H. Syed[1], Kent O. Kirlikovali[1], Christopher H. Hendon[3,4,*], Omar K. Farha[1,2,*]

[1]Department of Chemistry and International Institute for Nanotechnology, Northwestern University, Evanston, IL 60208, United States of America

[2]Department of Chemical and Biological Engineering, Northwestern University, Evanston, IL 60208, United States of America

[3]Department of Chemistry and Biochemistry, University of Oregon, Eugene, OR 97403, United States of America

[4]Materials Science Institute, University of Oregon, Eugene, OR 97403, United States of America

*Correspondence: chendon@uoregon.edu (Christopher H. Hendon), o-farha@northwestern.edu (Omar K. Farha)

Abstract

Since the structure of supramolecular isomers determines their performance, rational synthesis of a specific isomer hinges on understanding the energetic relationships between isomeric possibilities. To this end, we have systematically interrogated a pair of uranium-based metal–organic framework topological isomers both synthetically and through density functional theory (DFT) energetic calculations. Although synthetic and energetic data initially appeared to mismatch, we assigned this phenomenon to the appearance of a metastable isomer, driven by levers defined by Le Châtelier's principle. Identifying the relationship between structure and energetics in this study reveals how non-equilibrium synthetic conditions can be used as a strategy to target metastable MOFs. Additionally, this study demonstrates how defined MOF design rules may enable access to products within the energetic phase space which are more complex than conventional binary (e.g., kinetic vs. thermodynamic) products.

Table of Contents

Materials

Caution! Uranium salts are radioactive chemicals and contain depleted uranium (^{238}U). Necessary precautions must be adhered to when handling uranium salts.

All chemicals were purchased from the supplier and used without further purification. Tetraphenylmethane (Sigma-Aldrich), sodium hydroxide (Sigma-Aldrich), bromine (Sigma-Aldrich), ethanol (Fisher Scientific), chloroform (Fisher Scientific), Xantphos (Sigma-Aldrich), *N*-formylsaccharin (TCI America), potassium fluoride (anhydrous, Acros Organics), palladium(II) acetate (trace metal basis, Acros Organics), *N,N*-dimethylformamide (DMF, anhydrous, DriSolv, Millipore Sigma), and triethylamine (Fisher Scientific) were used to make the **TCPM** linker. Other chemicals used herein include uranyl nitrate hexahydrate (International Bio-Analytical Industries Inc.), formic acid (Millipore Sigma), DMF (Fisher Scientific), ethanol (Fisher Scientific), acetonitrile (Fisher Scientific), acetone (Fisher Scientific), sulfuric acid-d_2 (Millipore Sigma), dimethyl sulfoxide-d_6 (Millipore Sigma), and dimethylamine solution 40 wt. % in H_2O (Millipore Sigma).

Instrumentation

Imaging

Optical images were acquired with a Nikon SMZ1500 microscope.

Single Crystal X-ray Diffraction (SCXRD)

A NU-1306 single crystal was mounted using paratone oil and a MiTeGen loop onto a Rigaku XtaLAB Synergy diffractometer equipped with a micro-focus sealed X-ray tube PhotonJet (Cu) X-ray source and a Hybrid pixel Array detector (HyPix). The temperature of the crystal, set to 273.15K, was controlled with an Oxford Cryosystems low-temperature device. Data reduction was performed with the CrysAlisPro software using an empirical absorption correction with spherical harmonics. Using Olex2, the structure was solved with the SHELXT structure solution program using intrinsic phasing. The model was refined with ShelXL using least-squares minimization.

Powder X-ray Diffraction (PXRD)

PXRD data were obtained using a Stoe STADI P diffractometer, equipped with a CuKα1 source and a 1D strip detector. Transmission mode was used for all samples. Samples were prepared for PXRD by removing the DMF solvent, washing with fresh ethanol two times, and dropcasting onto the sample holder.

Nuclear Magnetic Resonance (NMR) Spectroscopy

^1H spectra of **TCPM** linker were collected on an A600, Bruker Avance III 600 MHz or an Au400, Bruker Avance III HD Nanobay 400 MHz instrument. ^1H spectra of digested MOFs were collected on an A600, Bruker Avance III 600 MHz instrument.

Supercritical CO_2 (sc-CO_2) Activation

Activation with sc-CO_2[1] was performed on a Tousimis Samdri PVT-3D critical point dryer, using a bone-dry CO_2 syphon tank. We followed a previously reported procedure.[2]

Gas Chromatography-Flame Ionization Detection (GC-FID)

CO and CO_2 separation and analysis were performed using an Agilent 7890A GC equipped with an FID. An aliquot of 0.5 mL sample gas was manually injected directly into an Agilent HP-Plot-Q column (19095P-QO4, Inner Diameter: 0.53 mm, Length: 30 m, Film Thickness: 40 μm) *via* a

split/splitless inlet using a Hamilton 1750 SL Gastight syringe equipped with Sample Lock. The detector was equipped with an ARC Jetanizer methanizer jet to allow for the detection of CO and CO_2. A second split/splitless inlet was used to maintain the flow of carrier gas through the HP-Molesieve column. The entire method was isothermal (T=35 °C) and used nitrogen as a carrier gas set to 4 mL. CO and CO_2 gas-phase species were identified using calibration standards with retention times of 1.88 and 2.93 minutes, respectively. Samples were prepared in Biotage 0.5-2 mL vials and crimped caps equipped with septa.

Thermal Activation

Thermal activation was performed under ultrahigh vacuum at 120 °C for 18 hours using a Micromeritics Smart VacPrep (SVP) instrument.

Thermogravimetric Analysis (TGA)

TGA experiments were performed using a TGA/DSC 1 LF (Mettler Toledo) instrument with STARe (v16.10) software. Samples were loaded into a 100 µL aluminum pan, heated from 30 °C to 120 °C, held at 120 °C for 1 hour, cooled from 120 °C to 30 °C, and heated from 30 °C to 600 °C. All ramp rates were performed at 5 °C/min in air.

Syntheses

Tetrakis(4-carboxyphenyl)methane (**TCPM**):

First, tetrakis(4-bromophenyl)methane (Scheme S1, **2**) was synthesized. To a 500 mL two-neck round bottom flask, equipped with a magnetic stir bar, we installed an outlet adaptor connected *via* rubber tubing to a pipette that was immersed in a solution of sodium hydroxide (20%, 250 mL). Tetraphenylmethane (10 g, 31.21 mmol) (Scheme S1, **1**) was then added to the flask. Next, neat bromine (11.1 mL, 216.64 mmol) was slowly added with continuous stirring at room temperature. The resultant, dark orange slurry was stirred for 25 min. Following this, 200 mL of ethanol, cooled to -78 °C, was added to the flask, and the suspension was sonicated and filtered. Precipitated material was then sonicated in 200 mL of saturated sodium sulfite solution and isolated by filtration. The crude product was then purified *via* recrystallization by solubilizing in 500 mL of a 1:1 mixture of boiling ethanol/chloroform followed by cooling in a freezer for 30 min. The compound was then filtered and dried to afford 13.9 g (70% yield).

TCPM was then synthesized based on a modified procedure from the literature (Scheme S1, **3**).[3] To an oven-dried, 200 mL heavy wall pressure vessel from Chemglass in a glovebox under Ar atmosphere, we added Xantphos (468.8 mg, 0.81 mmol) and palladium (II) acetate (121.2 mg, 0.54 mmol), followed by approximately 75 mL of anhydrous *N,N*-dimethylformamide (DMF). The Xantphos/Pd mixture was periodically swirled at room temperature while the remaining reagents were measured out. Next, tetrakis(4-bromophenyl)methane (2.21 g, 3.47 mmol) and potassium fluoride (2.62 g, 45.1 mmol) were added to the reaction flask. Lastly, *N*-formylsaccharin (4.75 g, 22.5 mmol) was added, resulting in effervescence. The reaction flask was quickly capped with a back seal solid PTFE bushing, equipped with a viton o-ring, and removed from the glovebox, after which it was vigorously stirred at 80 °C for approximately 3 days. After cooling to room temperature, 21 mL of triethylamine and 20 mL of deionized water were added to the reaction mixture, and it was stirred at room temperature for at least overnight. Following this, the volatiles were removed *in vacuo*. The crude product was then suspended in deionized water *via* sonication and isolated *via* vacuum filtration. After, it was suspended in 1 M NaOH (*aq*), and insoluble, dark solids were removed *via* vacuum filtration. The filtrate was next acidified with HCl to approximately pH = 1, and the precipitated product was collected from the aqueous solution *via* vacuum filtration. This precipitate was then dissolved in 1 M NaOH (*aq*) and passed through a Supor® 100

membrane disc filter (Pall, 0.1 µm – 47 mm, plain), followed by acidification with HCl to approximately pH = 1. It was collected *via* vacuum filtration and dried in a vacuum oven at 85 °C for 1-2 days, affording 1.56 g of a white solid (91% yield) (Fig S1).

NU-1305 Single Crystals

Single crystals of NU-1305 were synthesized by combining 0.5 mL (9.958 µmol) of a 10 mg mL^{-1} (19.915 mM) uranyl nitrate hexahydrate solution in N,N-dimethylformamide (DMF), 0.306 mL (6.164 µmol) of a 10 mg mL^{-1} (20.1422 mM) **TCPM** solution in DMF, and 30 µL of formic acid (FA) in a 1.5 dram glass vial. The mixture was sealed in the glass vial, sonicated for 2 minutes, and placed in a 120 °C oven for 24 hours. Large 200 µm tetrahedrally-shaped yellow crystals were observed on the bottom and walls of the vial that were submerged in solvent (Fig S2).

NU-1306 Single Crystals

Single crystals of NU-1306 were synthesized by combining 0.5 mL (9.958 µmol) of a 10 mg mL^{-1} (19.915 mM) uranyl nitrate hexahydrate solution in N,N-dimethylformamide (DMF), 0.306 mL (6.164 µmol) of a 10 mg mL^{-1} (20.1422 mM) **TCPM** solution in DMF, and 25 µL of formic acid (FA) in a 1.5 dram glass vial. The mixture was sealed in the glass vial, sonicated for 2 minutes, and placed in a sand-bath in a 45 °C oven for 72 h (the resulting solution was still clear). The vial was then left undisturbed at room temperature for 14 weeks. Large tetrahedrally-shaped yellow crystals were observed on the bottom and walls of the vial that were submerged in solvent, similar to those of NU-1305. Additional block-shaped crystals were also observed on the headspace walls of the vial (Fig S3). A selected 78 x 100 x 117 µm block crystal diffracted to reveal the structure of NU-1306. Data collection and refinement details are included in Table S1. The asymmetric unit, node coordination, and pore sizes can be found in Figure S5. PLATON was used to calculate 84% solvent accessible pore volume.

Bulk Syntheses Varying Modulator Ratio

NU-1305 and NU-1306 were synthesized by varying the modulator ratio in the following manner. 0.5 mL (9.958 µmol) of a 10 mg mL^{-1} (19.915 mM) uranyl nitrate hexahydrate solution in DMF and 0.306 mL (6.164 µmol) of a 10 mg mL^{-1} (20.1422 mM) **TCPM** solution in DMF were combined in a 1.5 dram glass vial. Either 25, 40, 50, 70, 80, 90, 100, or 120 µL of FA was added to the linker and node mixture. We define each modulator amount by the volumetric ratio of FA to DMF (0.806 mL total) such that samples with 25 µL FA are 0.03 FA:DMF, 40 µL FA are 0.05 FA:DMF, 50 µL FA are 0.06 FA:DMF, 70 µL FA are 0.09 FA:DMF, 80 µL FA are 0.10 FA:DMF, 90 µL FA are 0.11 FA:DMF, 100 µL FA are 0.12 FA:DMF, and 120 µL FA are 0.15 FA:DMF. Each mixture was sealed in its glass vial, sonicated for 2 minutes, and placed in a 120 °C oven. Samples with 0.03 FA:DMF remained in the oven for 24 h, 0.05 and 0.06 FA:DMF for 48 h, 0.09 FA:DMF for 7 days, 0.10, 0.11, and 0.12 FA:DMF for 5 days, and 0.15 FA:DMF for 6 days. All samples with a FA:DMF ratio at or below 0.09 resulted in NU-1305, and all samples with a FA:DMF ratio at or above 0.10 resulted in NU-1306.

Bulk Syntheses Varying Temperature

NU-1305 and NU-1305 were synthesized by varying the reaction temperature in the following manner. 0.5 mL (9.958 µmol) of a 10 m gmL^{-1} (19.915 mM) uranyl nitrate hexahydrate solution in DMF, 0.306 mL (6.164 µmol) of a 10 m gmL^{-1} (20.1422 mM) **TCPM** solution in DMF, and 70 µL FA (11.5 DMF:FA) were combined in a 1.5 dram glass vial. The mixture was sealed in the glass vial and sonicated for 2 minutes. Samples were placed in either a 120 °C oven for 24 h, a 160 °C for 6 h, or a 170 °C oven for 1 h. Samples run at 170 °C were wrapped in Teflon tape to slow down solvent loss. Samples at 120 °C resulted in NU-1305, 160 °C in a mixture of both isomers, and 170 °C in NU-1306. When the 170 °C synthesis was performed in a sealed pressure reaction

vessel, black product (Fig S6a) appearing amorphous by PXRD (Fig S6b) was observed. When the 120 °C synthesis was performed in a sealed pressure reaction vessel, NU-1305 was still observed (Fig S6c).

Bulk Syntheses Varying Reaction Concentration

NU-1305 and NU-1306 were synthesized by varying the reaction concentration in the following manner. 0.5 mL (9.958 µmol) of a 10 mg mL^{-1} (19.915 mM) uranyl nitrate hexahydrate solution in DMF, 0.306 mL (6.164 µmol) of a 10 mg mL^{-1} (20.1422 mM) **TCPM** solution in DMF, and 80 µL FA (0.10 FA:DMF) were combined in a 1.5 dram glass vial. Either 0, 0.25, 0.5, 0.75, or 1 mL of additional DMF was added to the linker and node mixture. We define each reaction by its total volume. Thus, samples with 0 mL added DMF have a 0.8 mL total volume, 0.25 mL added DMF have a 1.1 mL total volume, 0.5 mL added DMF have a 1.3 mL total volume, 0.75 mL added DMF have a 1.6 mL total volume, and 1 mL added DMF have a 1.8 mL total volume. Each mixture was sealed in its glass vial, sonicated for 2 minutes, and placed in a 120 °C oven for 6 days. Samples with 0.8 and 1.1 mL total volume resulted in NU-1306 while samples with a total volume at or above 1.3 gradually possessed less NU-1306 and more NU-1305.

The same reactions were run with 70 µL FA instead (0.09 FA:DMF) diluted to either 1.8 total mL (48h reaction time) or concentrated to 0.4 total mL (24h reaction time) (Fig S7).

Conversion of NU-1305 to NU-1306

NU-1305 was converted to NU-1306 by first soaking synthesized NU-1305 in fresh DMF for one hour and repeating this procedure three times. Then, 5 mg of NU-1305, 1 mL fresh DMF, and 200 µL FA were added to a 1.5 dram vial, sealed, and placed in a 170 °C oven for 3.5 h. The resulting solid was identified as NU-1306 by PXRD (Fig S8). Attempting conversion at less harsh conditions resulted in no observed conversion to NU-1306.

Conversion of NU-1306 to NU-1305

NU-1306 was converted to NU-1305 by first soaking synthesized NU-1306 in fresh DMF for one hour and repeating this procedure three times. Conversion was accomplished using two sets of conditions. The first condition involved combining 5 mg of NU-1306, 1 mL fresh DMF, and 25 µL FA in a 1.5 dram vial. The vial was then sealed and placed in a 170 °C oven for 1 h. The second condition involved combining 5 mg of NU-1306, 1 mL fresh DMF, and 70 µL FA in a 1.5 dram vial. The vial was then sealed and placed in a 120 °C oven for 3 days. The resulting solids from both sets of conditions were identified as NU-1305 by PXRD (Fig S9). Attempting conversion at less harsh conditions resulted in no observed conversion to NU-1305.

Counterion Analysis

Since NU-1305 and NU-1306 are anionic MOFs, we expect that either dimethylammonium (from the degradation of DMF), H^+, or H_3O^+ act as counterbalancing cations. To search for the presence of dimethylammonium, we implemented ^{1}H NMR analysis. NU-1305 and NU-1306 were each prepared by first washing in fresh acetonitrile and exchanging the acetonitrile once every hour for three hours. Samples were then soaked in acetonitrile overnight (~16 hours) and activated *via* sc-CO_2 activation. Approximately 2-3 mg of activated MOF was sonicated in five drops of sulfuric acid-d_2, diluted to approximately 0.5 mL with dimethyl sulfoxide-d_6, and sonicated again. ^{1}H NMR spectra of NU-1305 (Fig S10) and NU-1306 (Fig S11) was integrated per node (0.75 linkers per node), and doublets at 7.22 and 7.77 ppm are assigned to the **TCPM** linker. We did not observe any peaks for dimethylammonium in either sample. A control experiment of dimethylamine treated under the same digestion conditions shows peaks for dimethylammonium at 2.8 and 2.9 ppm (3:1

integration, respectively). Comparing this spectrum to those of NU-1305 and NU-1306 confirms that dimethylammonium is not present in either sample (Fig S12). Thus, we deduce that either H^+ or H_3O^+ act as counterbalancing cations, similar to results we have reported previously. [2]

Geometric Analysis

Node Geometry Analysis

The node geometry was measured in Mercury by first calculating the plane which includes a uranium atom and the two oxygen atoms from an equatorially bound linker (plane A). The plane holding the immediately bound linker phenyl ring was also calculated (plane B). We then measured the angle between the two planes for both NU-1305 and NU-1306, which was 1.25° and 9.57°, respectively (Fig S13).

Linker Geometry Analysis

Linker geometry was analyzed in Mercury by measuring the linker dihedral angles for NU-1305 and NU-1306 (Fig S14). There are six total dihedral angles per linker, listed in Table S2. While both MOF linkers had similar mean dihedral angle values, the standard deviation of these angles from the mean differed significantly, showing that the angle range and distortion in NU-1306 is larger than that of NU-1305. (Table S2).

Crystal Density

Crystal density was measured in CrystalMaker. The density of NU-1306 lies at 0.470 g cm^{-3} while that of NU-1305 is 0.521 g cm^{-3}.

DFT Calculations

Beginning with the experimentally collected crystallographic positions, the cell parameters of both the **bor** and **ctn** structures were geometrically equilibrated using VASP. The geometries were obtained using a 500 eV planewave cutoff, a 2 x 2 x 2 k-grid, paired with the PBEsol functional. Energy was converged to within 0.005 eV per atom. The computational lattice constants *a*=*b*=*c* were found to be 20.98 Å, and 32.20 Å for **bor** (NU-1306) and **ctn** (NU-1305), respectively. These values were in excellent agreement with the experimental values of 20.90 Å and 32.12 Å for the **bor** (NU-1306) and **ctn** (NU-1305) structures, respectively. The calculated axial and equatorial U-O bond lengths for both polymorphs are similar to the experimental values and can be found in Table S3. The computational structures are included in the supporting data as CIFs. To obtain higher level electronic structure information (density of states, bond energies, accurate comparison of isomer energies) single point HSE06 calculations were performed on the equilibrium structures.[4] These energies were compared, and the lowest energy isomer was deduced by normalizing for differences in cell size. A background charge was applied to correct the oxidation state of each MOF in order to compensate for the existence of hydronium contained within the pores. The work functions were obtained using the ΔSCF method. A summary of the computational findings is presented in Figure S15.

To compare the energetics of the linkers and nodes, the linker and node geometries were extracted from the equilibrium structures. The linkers were then computed as the tetra-anion without optimization in Gaussian09, using HSE06 and a triple zeta polarized basis. The nodes were computed with passivating formates added. The U-O bond lengths were not allowed to relax, but the C-O and C-H bonds were allowed to reach equilibrium. This approach maintained

the local coordination environment of the node within the MOF, while also maintaining the local symmetry around the U-centers.

Gas Chromatography Measurements

We analyzed the byproducts of the NU-1305 and NU-1306 reactions using gas chromatography (GC). Pathway 1 in Equation 1 can be distinguished by the presence of CO, and pathway 2 by the presence of CO_2. Thus, we analyzed the headspace of the NU-1305 and NU-1306 reactions for CO and CO_2 to determine if one or both pathways are operative.

For the 120 °C NU-1305 synthesis at 0.03 FA:DMF, GC measurements were taken at a 7-hour timepoint and after completion of the reaction. Both CO and CO_2 were observed at 7 hours and after reaction completion, suggesting that both pathways 1 and 2 are operative in NU-1305 formation under these conditions (Fig S16). By integrating the area under each peak, we observed a CO_2:CO ratio of 10.5:1 at 7 hours and 5.4:1 at reaction completion. This data indicates that pathway 2 dominates for the entirety of the reaction and that formic acid degradation through pathway 1 increases over the course of the reaction (while still not usurping pathway 2).

For the 120 °C NU-1306 synthesis at 0.15 FA:DMF, GC measurements were taken at a 31-hour timepoint and after completion of the reaction. Similar to NU-1305, both CO and CO_2 were observed at 31 hours and after reaction completion, suggesting that both pathways 1 and 2 are operative in NU-1306 formation under these conditions (Fig S17). By integrating the area under each peak, we observed a CO:CO_2 ratio of 1.6:1 at 31 hours and 3.6:1 after reaction completion. This data indicates that pathway 1 dominates for the entirety of the reaction and that formic acid degradation through pathway 2 decreases over the course of the reaction (while still not usurping pathway 1).

Thus, while both pathways are present for the two isomer MOF syntheses, pathway 1 dominates for NU-1306 synthesis while pathway 2 dominates for NU-1305 synthesis.

Missing Linker Analysis

Missing linker was determined using TGA. A blank sample was measured to account for thermal expansion upon heating, and this trace was subtracted from all sample traces. Using $H^+[UO_2(\mathbf{TCPM})_{0.75}]^-$ as the formula of the starting material and U_3O_8 as the material remaining after the TGA measurement, we calculated an expected 56.3% linker for both NU-1305 and NU-1306. TGA data shows a general trend of decreasing linker present with increasing modulator amount (Fig S18), revealing an increasing percentage of missing linker with increasing modulator (Table S4).

Supplementary Tables, Schemes, and Figures

Table S1. Single crystal data and structure refinement details for NU-1306.

	NU-1306
Empirical formula	$C_{87}H_{48}O_{32}U_4$
Formula weight	2557.37
Temperature/K	273.15
Crystal system	cubic
Space group	P-43m
a/Å	20.90200(10)
b/Å	20.90200(10)
c/Å	20.90200(10)
α/°	90
β/°	90
γ/°	90
Volume/Å^3	9131.95(13)
Z	1
ρ_{calc}g/cm^3	0.465
μ/mm^{-1}	5.098
F(000)	1194.0
Crystal size/mm^3	0.078 × 0.100 × 0.117
Radiation	CuKα (λ = 1.54178)
2Θ range for data collection/°	4.228 to 144.008
Index ranges	-25 ≤ h ≤ 24, -25 ≤ k ≤ 19, -14 ≤ l ≤ 25
Reflections collected	33250
Independent reflections	3351 [R_{int} = 0.0388, R_{sigma} = 0.0146]
Data/restraints/parameters	3351/2/57
Goodness-of-fit on F^2	1.114
Final R indexes [I>=2σ (I)]	R_1 = 0.0668, wR_2 = 0.1786
Final R indexes [all data]	R_1 = 0.0695, wR_2 = 0.1825
Largest diff. peak/hole / e Å^{-3}	1.53/-1.73
Flack parameter	0.027(12)

Table S2. Linker dihedral angles, measured in degrees. Refer to Figure S14 for atom labels.

Angle	**NU-1305**	**NU-1306**
C1a-C6-C1b	112.6	118.8
C1a-C6-C1c	112.6	118.8
C1a-C6-C1d	103.3	92.2
C1b-C6-C1c	112.6	92.2
C1c-C6-C1d	112.6	118.8
C1d-C6-C1b	103.3	118.8
Mean	109.5	110.0
St. Dev.	4.4	12.5

Table S3. Node bond lengths from experimental and geometry-optimized structures.

MOF	Experimental		Calculated	
	U-O_{axial} (Å)	U-O_{equ} (Å)	U-O_{axial} (Å)	U-O_{equ} (Å)
NU-1305	1.78	2.42 (50%)* 2.41 (50%)*	1.80	2.47
NU-1306	1.80	2.45	1.80	2.47

*Equatorial bond lengths in the experimental structure of NU-1305 are 2.42 Å 50% of the time and 2.42 Å 50% of the time.

Table S4. Percent missing linker for NU-1305 and NU-1306 synthesized at different FA:DMF ratios.

FA:DMF	Missing Linker (%)
0.03	0
0.05	0
0.06	1.2
0.09	1.1
0.10	7.4
0.11	9.3
0.12	10.1
0.15	10

Scheme S1. Synthesis of tetrakis(4-carboxyphenyl)methane

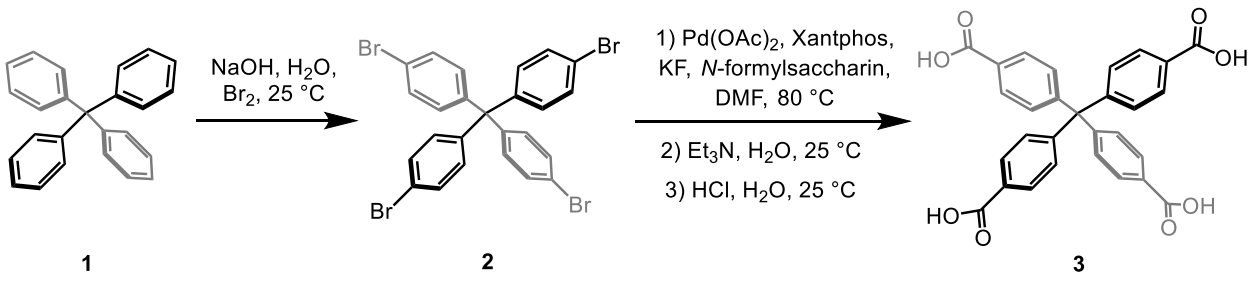

1 2 3

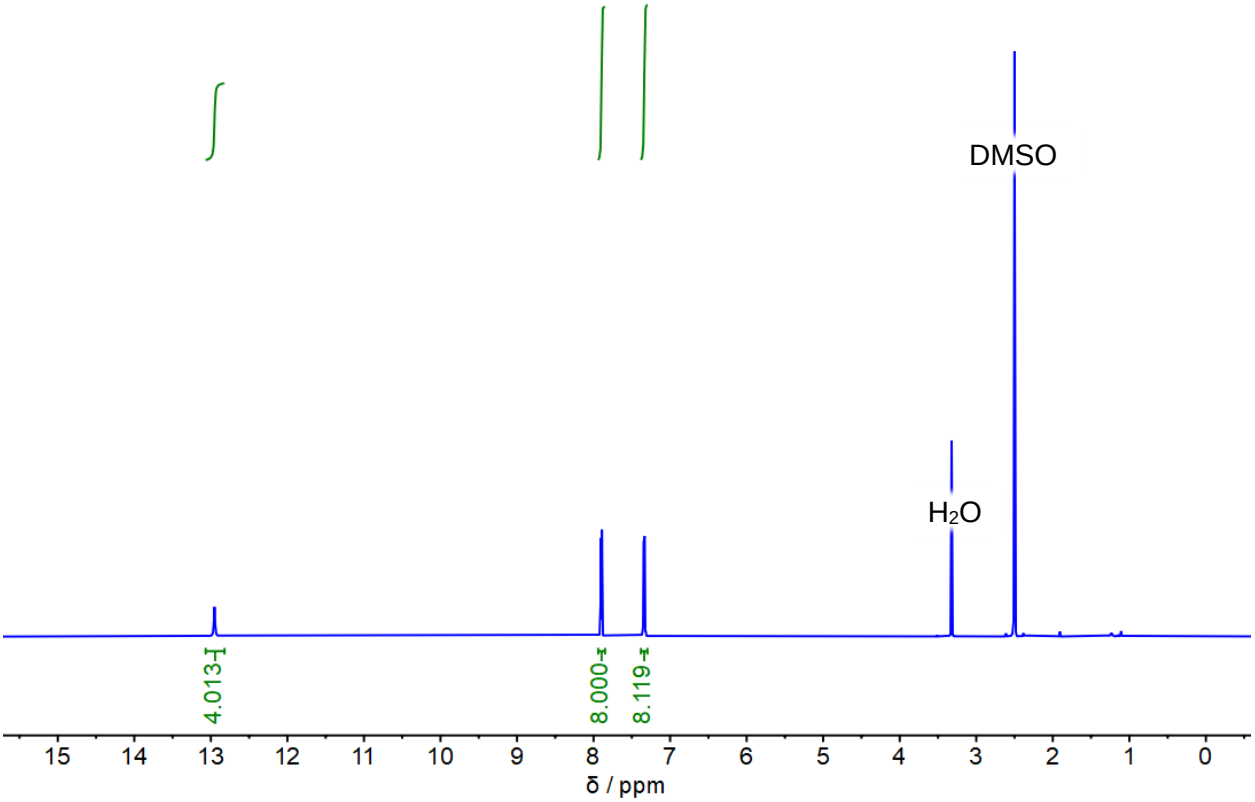

Figure S1. ^{1}H NMR spectra of **TCPM** in dimethyl sulfoxide-d_6 (DMSO).

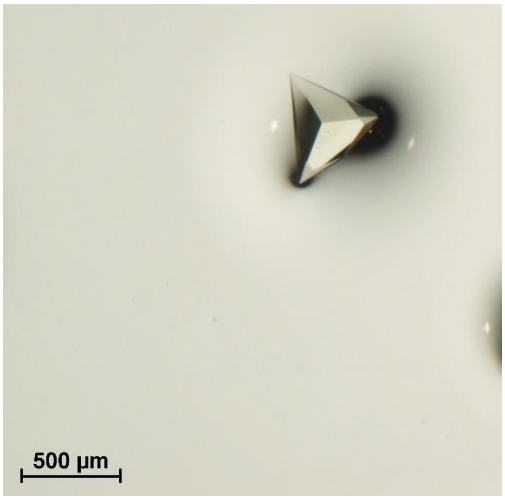

Figure S2. Optical image of NU-1305 single crystal.

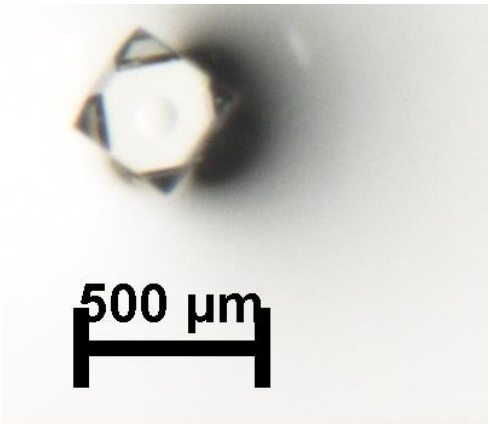

Figure S3. Optical image of NU-1306 single crystal.

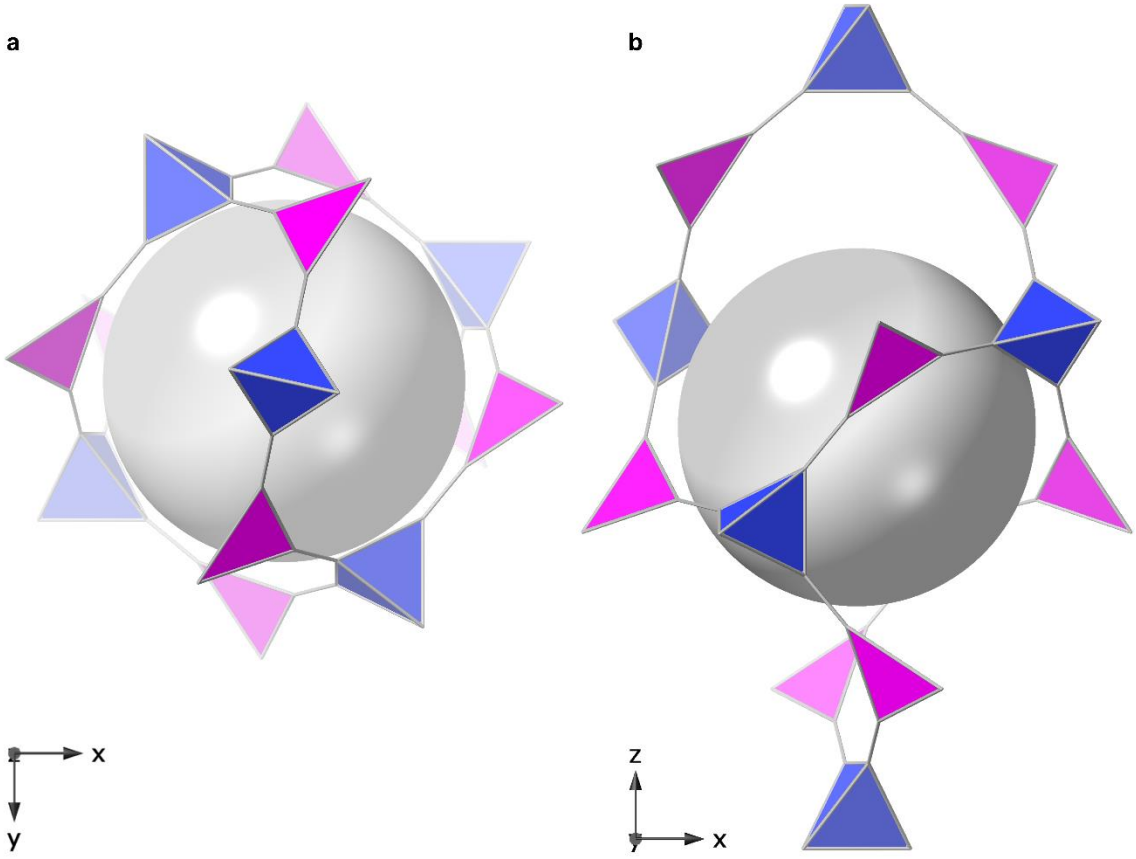

Figure S4. Augmented crystal structure and pore size of NU-1305 down the (**a**) z and (**b**) y axes.

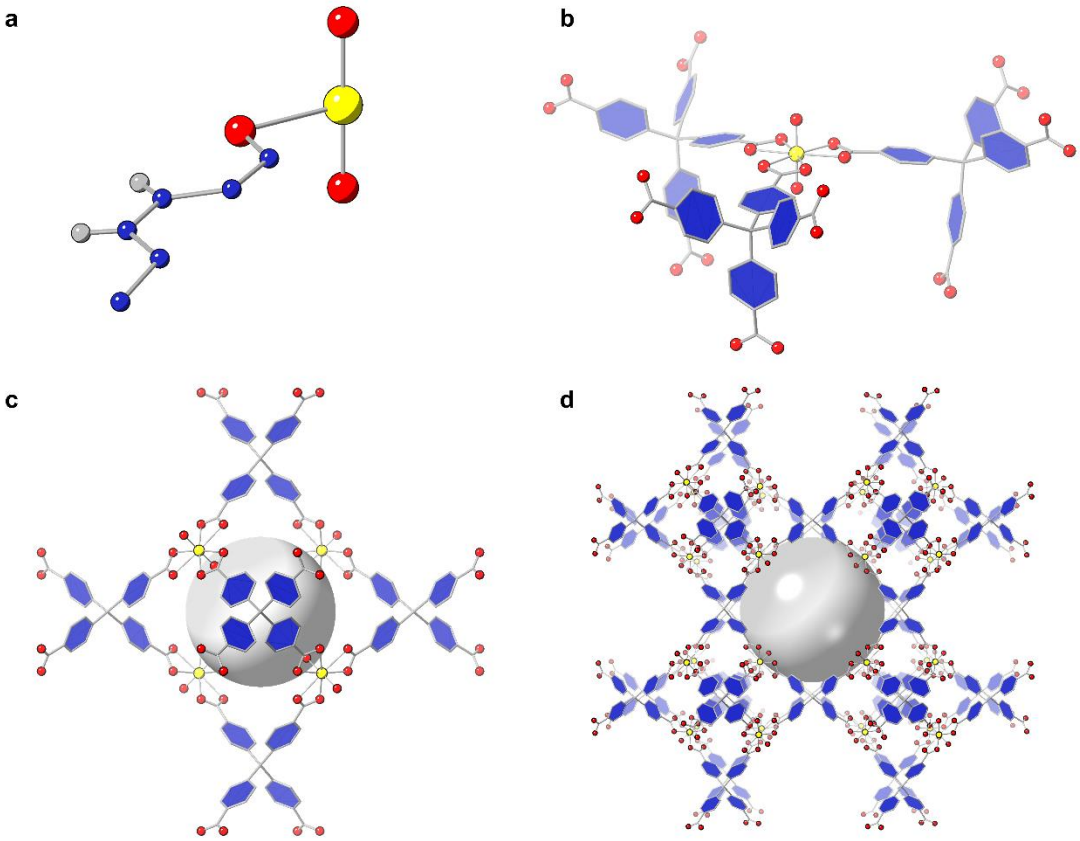

Figure S5. NU-1306 (**a**) asymmetric unit, (**c**) 12.8 Å radii octahedral cages, and (**d**) 22 Å radii apertures. (**b**) Node coordination of both NU-1305 and NU-1306. Uranium is shown in yellow, oxygen in red, and carbon in blue. Hydrogen atoms are omitted in all panels, but they are shown in grey in panel **a** for clarity.

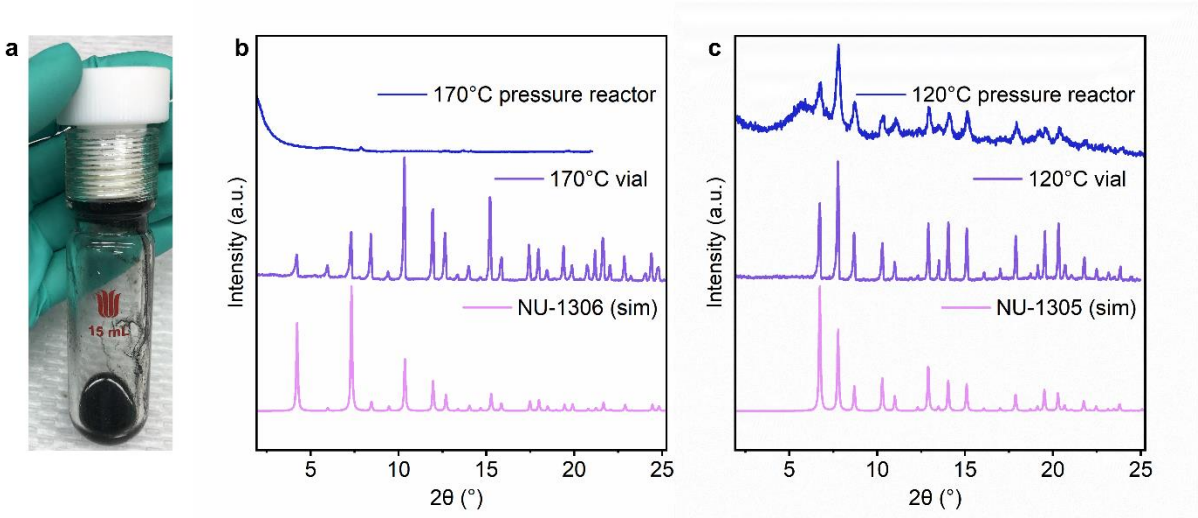

Figure S6. (**a**) Black product from 170 °C reaction in pressure reactor. PXRDs of (**b**) NU-1306 and (**c**) NU-1305 syntheses in pressure reactors and glass vials compared to their respective simulated patterns.

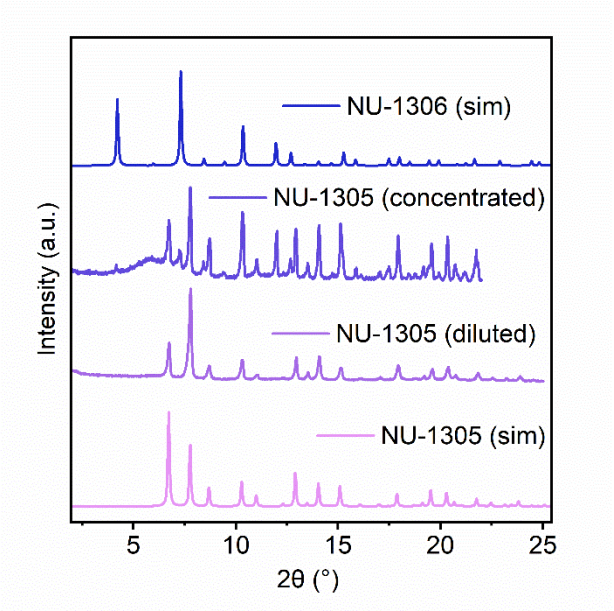

Figure S7. Results of diluting (total volume of 1.8 mL) and concentrating (total volume of 0.4 mL) the initial synthesis that formed NU-1305 (0.09 FA:DMF, 0.8 mL DMF, 120 °C).

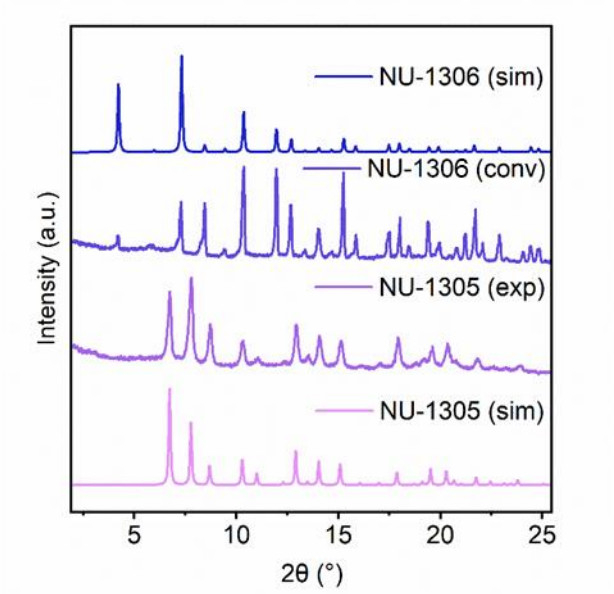

Figure S8. PXRD showing conversion of NU-1305 to NU-1306. From bottom to top: simulated NU-1305, experimental NU-1305, experimental NU-1305 converted to NU-1306, and simulated NU-1306.

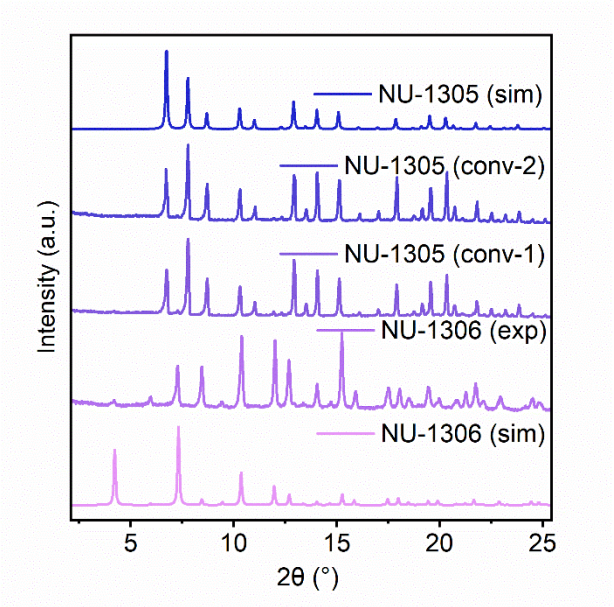

Figure S9. PXRD showing conversion of NU-1306 to NU-1305. From bottom to top: simulated NU-1306, experimental NU-1306, experimental NU-1306 converted to NU-1305 under condition one, experimental NU-1306 converted to NU-1305 under condition two, and simulated NU-1305.

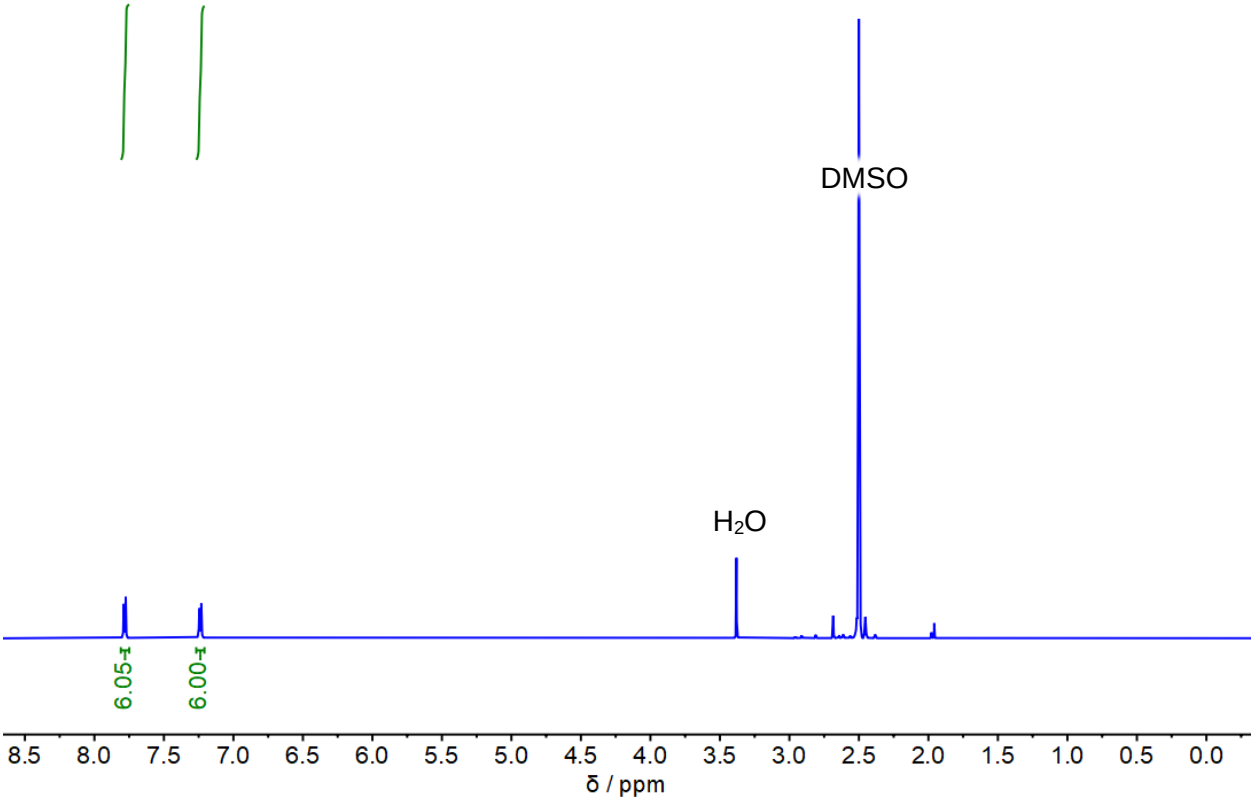

Figure S10. ^{1}H NMR spectra of acid-digested NU-1305 in dimethyl sulfoxide-d_6 (DMSO).

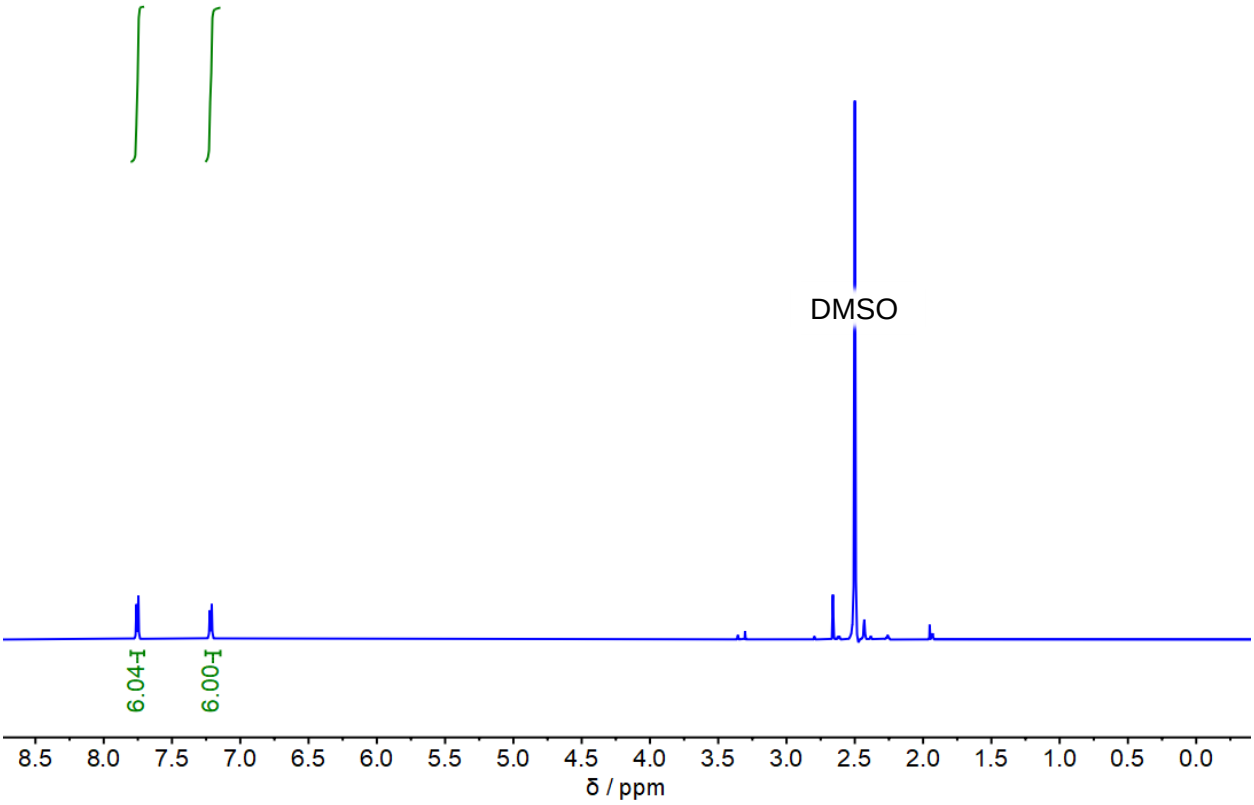

Figure S11. ^{1}H NMR spectra of acid-digested NU-1306 in dimethyl sulfoxide-d_6 (DMSO).

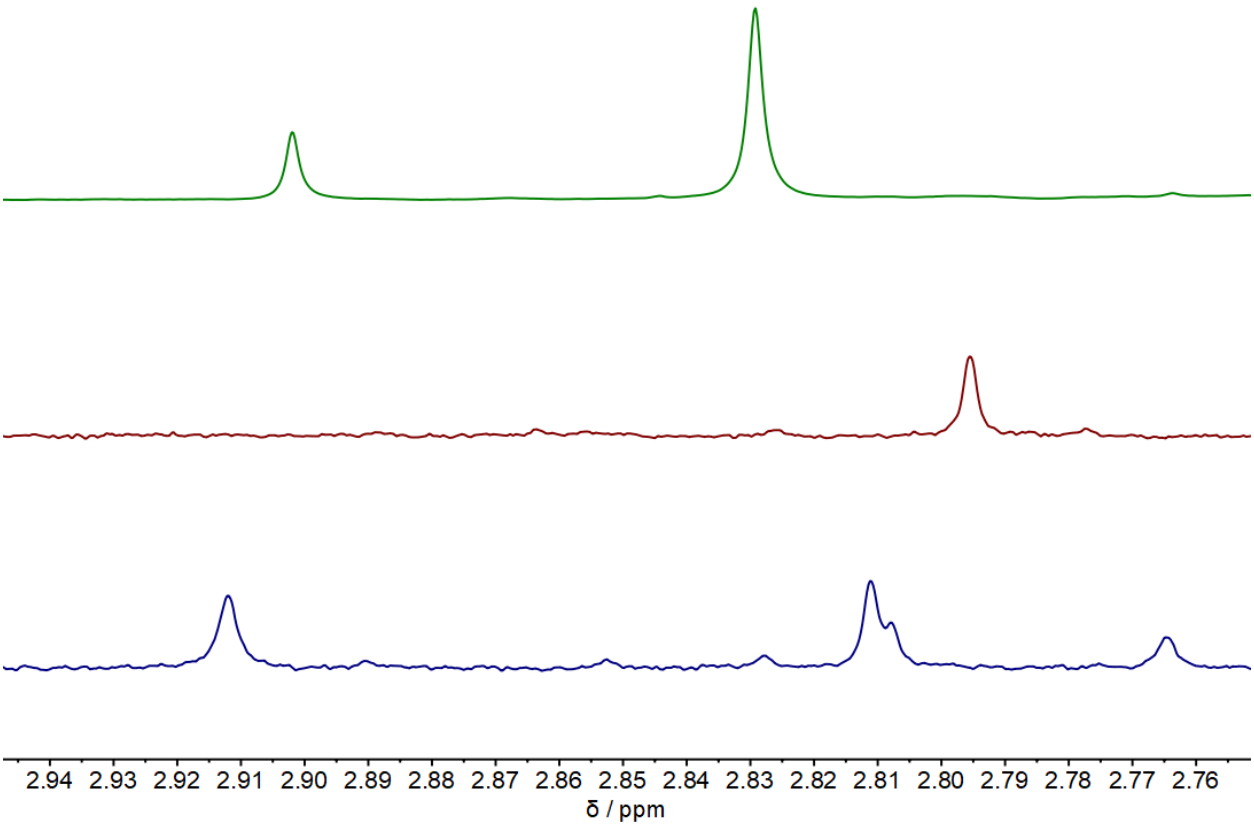

Figure S12. ^{1}H NMR spectra of dimethylamine (top) compared to acid-digested NU-1306 (middle) and acid-digested NU-1305 (bottom) in dimethyl sulfoxide-d_6 (DMSO).

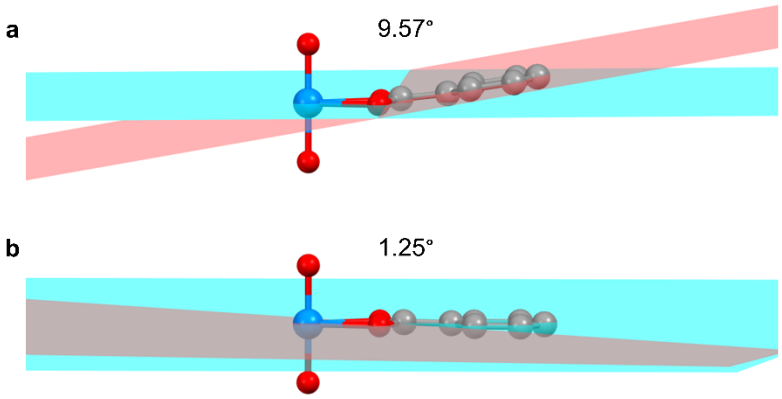

Figure S13. Geometric analysis of (**a**) NU-1306 and (**b**) NU-1305 nodes. Plane A is shown in aqua, and plane B is shown in red. Uranium is shown in blue, oxygen in red, and carbon in gray. Hydrogen atoms are omitted for clarity.

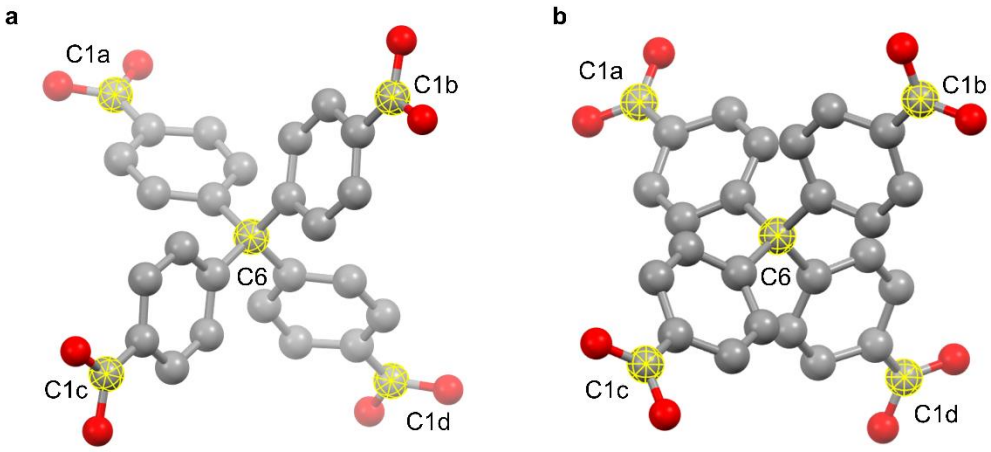

Figure S14. Geometric analysis of (**a**) NU-1306 and (**b**) NU-1305 linkers. Yellow highlighted carbon atoms were used to measure dihedral angles in Table S2. Oxygen is shown in red and carbon in gray. Hydrogen atoms are omitted for clarity.

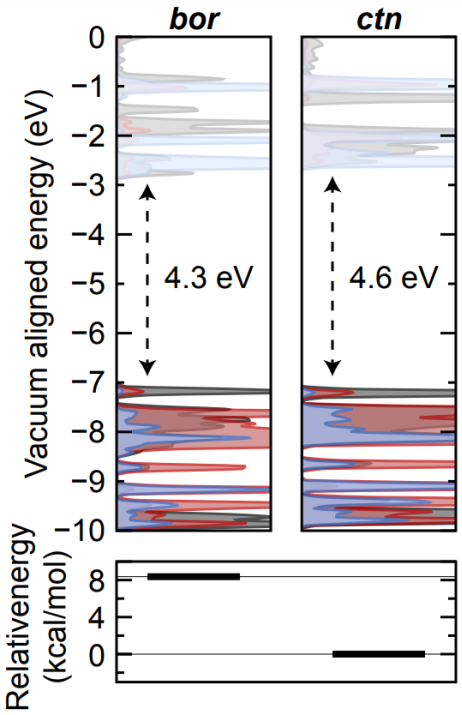

Figure S15. Summary of DFT results. The ctn (NU-1305) and bor (NU-1306) structures are predicted to have similar electronic properties (top), but ctn is 8 kcal mol^{-1} more stable than the bor topology (bottom).

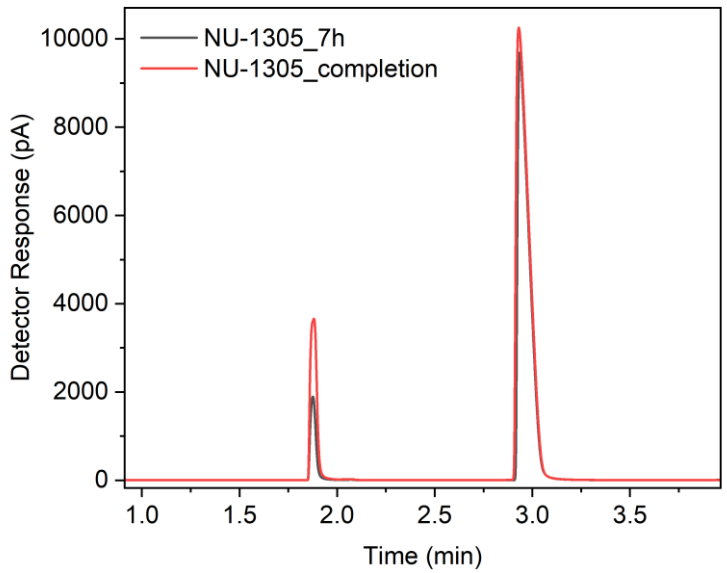

Figure S16. GC trace for NU-1305 synthesis. CO is observed at 1.88 minutes retention time and CO_2 at 2.93 minutes retention time.

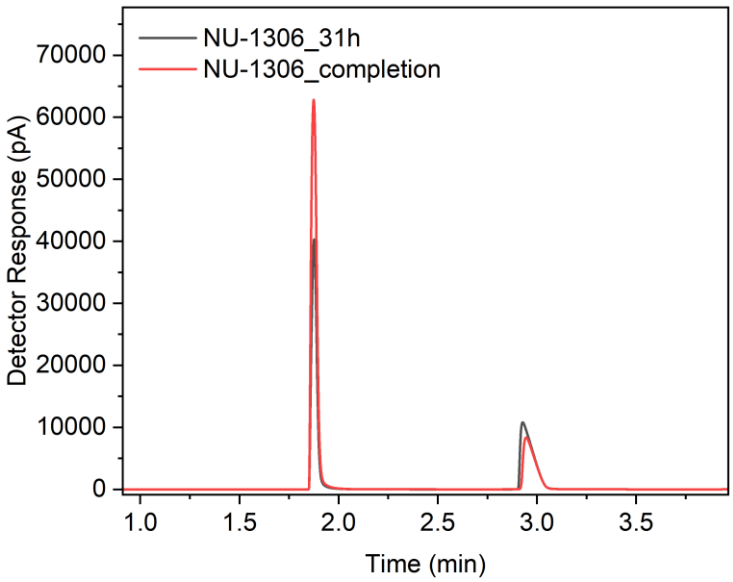

Figure S17. GC trace for NU-1306 synthesis. CO is observed at 1.88 minutes retention time and CO_2 at 2.93 minutes retention time.

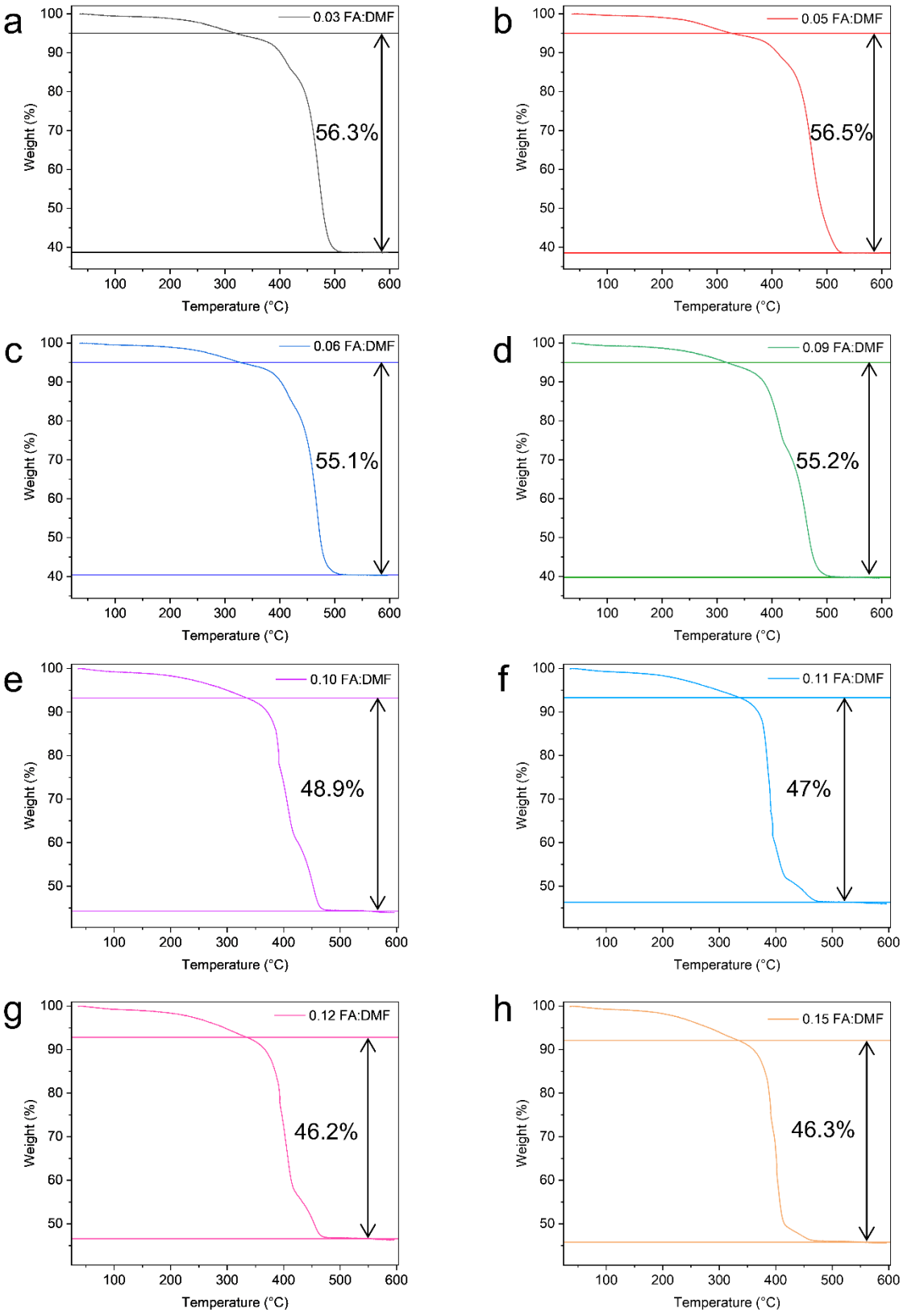

Figure S18. TGA data of NU-1305 (a-d) and NU-1306 (e-h) synthesized at different FA:DMF ratios.

References

1. A. P. Nelson, O. K. Farha, K. L. Mulfort and J. T. Hupp, *J. Am. Chem. Soc.*, 2009, **131**, 458-460.
2. S. L. Hanna, S. Chheda, R. Anderson, D. Ray, C. D. Malliakas, J. G. Knapp, K.-i. Otake, P. Li, P. Li, X. Wang, M. C. Wasson, K. Zosel, A. M. Evans, L. Robison, T. Islamoglu, X. Zhang, W. R. Dichtel, J. F. Stoddart, D. A. Gomez-Gualdron, L. Gagliardi and O. K. Farha, *Chem*, 2022, **8**, 225-242.
3. X. Zhang, Z. Huang, M. Ferrandon, D. Yang, L. Robison, P. Li, T. C. Wang, M. Delferro and O. K. Farha, *Nat. Catal.*, 2018, **1**, 356-362.
4. J. P. Perdew, M. Ernzerhof and K. Burke, *J. Chem. Phys.*, 1996, **105**, 9982-9985.